

Short-Range Interactions of Globular Proteins at High Ionic Strengths

Sabrina Beretta, Giuseppe Chirico,* and Giancarlo Baldini

*Istituto Nazionale per la Fisica della Materia, Università di Milano Bicocca, Via Celoria 16, I-20133 Milano, Italy**Received April 7, 2000; Revised Manuscript Received July 31, 2000*

ABSTRACT: We compare the interactions of betalactoglobulin and lysozyme under different salt concentrations of ammonium sulfate by means of photon correlation spectroscopy measurements. The diffusion coefficient depends linearly upon protein concentration (1–25 g/L), and no evident aggregation occurs even at the highest salt concentrations. The slope of the diffusion coefficient is larger for lysozyme than for betalactoglobulin, especially at high salt concentration. The analysis of the interaction coefficients by means of the DLVO theory does not offer an unified picture of the protein interactions for the two systems. We discuss the possibility that specific (hydrogen bonding, salt bridges, etc.) or nonspecific (hydration forces) interactions, that go beyond the DLVO approximation, might be the origin of the larger van der Waals attraction shown by lysozyme. The data are consistent with a contribution of repulsive hydration forces that are smaller for lysozyme than for betalactoglobulin. This effect is in agreement with the difference in the protein size and charge.

I. Introduction

The growth of protein crystals is the first and limiting step when determining a protein atomic structure by means of X-ray diffraction studies. Making protein crystals, however, is a difficult task contrary to what is found, for example, for hard-sphere colloids¹ whose crystallization is almost routine. Protein structural data are needed, for instance, for drug design, or for the understanding of genome structure–function correlations. The interest in protein crystallization and protein–protein interactions stems also from the observation that proteins crystallize and aggregate under physiological conditions and are responsible for severe pathological conditions.

Essential to the understanding of the growth of protein crystals is a detailed modeling of protein–protein interactions that occur in the aqueous solvent. In principle the description can be given atomistically, but the presence of the water hydrogen-bonded structure and the possibility for many of the protein residues to establish hydrogen bonding with the hydration water lead to a complexity which can be overcome only through molecular dynamics simulations.² This approach, on the other hand, can be successfully applied only to systems of small size and for short simulation times, a procedure that does not allow an easy and direct comparison to the experimental results. Consequently, one is often forced to use oversimplified models that treat the solvent as a continuum and the protein interactions as due to an effective spherical symmetric potential. Within this oversimplified framework, it is customary to treat the interactions and stability of colloids and globular proteins in terms of a composition of the van der Waals attraction and the electrostatic repulsion, through the DLVO (Derjaguin–Landau–Verwey–Overbeek) theory.³

The extent of the degree of approximation and simplification of this approach for a realistic description of the protein–protein interactions can be perceived from the observation of the highly ordered protein packing

in crystals. The mutual arrangement of the proteins in crystals requires some anisotropy^{4,5} in the short-range interactions which bring the molecules together. Few attempts have been made to account for anisotropy by means of the numerical simulations,² whereas several analytical approaches have been applied to colloidal and protein solutions in an attempt to identify and to test models that reproduce an effective spherical symmetric protein–protein interaction energy.^{3,6–9} Very recently theoretical studies of the phase diagrams of colloids with anisotropic interactions have been presented,^{5,10} and though the details of protein–protein interactions are poorly understood, a substantial contribution of specific and directional interactions at very short range is expected.¹¹ Furthermore, recent interest in non-DLVO interactions of proteins has been put forth on the basis of anomalous attractions at high salt content of the solutions,¹² even though in a mean-field approximation that cannot take into account the details of the protein–solvent interactions.

Despite the considerable experimental and theoretical work on the subject, the conditions yielding protein crystals are still tested through a virtual trial and error method.¹³ Few rules seem to exist: crystallization is frequently obtained by addition of electrolytes, such as NaCl or ammonium sulfate (NH₄)₂SO₄, or of nonadsorbing polymers,¹⁴ such as poly(ethylene glycol) (PEG), or glycerol.¹⁵ Protein solutions evolve toward amorphous aggregation more often than producing good quality crystals. Moreover the evolution of the protein solution depends critically on how rapidly the crystallization agent is added to the solution and on the temperature of the solution.¹⁶

In this paper, we give a critical analysis of the mean-field theoretical models usually employed for describing protein–protein interactions and point out the relevance of the very short-range interaction in determining the properties of protein solutions at high ionic strength. The experimental test is performed on two globular proteins of similar size and net charge, lysozyme and betalactoglobulin (BLG), in solutions of ammonium sulfate at different concentration. This salt is typically employed for betalactoglobulin crystallization, while

* Corresponding author. E-mail: Giuseppe.Chirico@mi.infm.it.

lysozyme is known to crystallize much more effectively in NaCl solutions. For this reason lysozyme is considered here as a reference system to which crystallizing betalactoglobulin can be compared. The investigation of the protein–protein interactions vs ionic strength for the two protein systems is performed by measuring the concentration dependence of the mutual diffusion coefficients when various amounts of salt are added to the solutions.

The main conclusion here is to have shown that a good parameter for the description of the interaction properties of the protein at high ionic strength should be sought in the amplitude of the short-range interactions (≤ 2 nm). We try to draw conclusions on the origin of the difference in the short-range interactions observed for the two proteins in terms of specific interactions such as hydrogen bonding or salt bridges or unspecific hydration interactions.¹⁷ The present data are consistent with larger hydration interactions between betalactoglobulin than between lysozyme induced by the condensation of hydrated positive counterions on betalactoglobulin.

II. Theoretical Considerations

A physical approach to protein crystallization has been suggested by George and Wilson¹⁸ who indicated a criterium to obtain good quality protein crystals based on whether the values of the second virial coefficient, B_2 , fall within a narrow range. Following this paper several recent studies^{12,15,19–21} of the protein–protein interactions in nearly-saturated and supersaturated solutions have shown that a short-range intermolecular attractive interaction is induced by the addition of salt or nonadsorbing polymers. The short-range nature of the protein–protein interaction and its anisotropy⁵ determines the existence of a metastable liquid–liquid–phase boundary below the liquid–solid boundary that corresponds to the normal crystallization (freezing). This behavior, common to various protein systems, corresponds to a phase separation into two amorphous phases, one depleted and one concentrated in protein.^{21,22}

Some works on the protein crystallization successfully model the protein–protein interactions by means of the adhesive-hard-sphere (AHS) potential energy⁷ that is a simple attractive rectangular well of vanishing interaction range.²³ This suggests again the presence of an extremely short-range attractive interaction with respect to the protein size, though the phase diagram that can be obtained from the AHS model does not fully describe the rich behavior of the protein solutions.²²

The role of the range of the attractive interactions in determining the phase diagram of protein solutions, has also been set forth by recent experimental studies on eye lens proteins²⁴ and on lysozyme¹⁶ together with recent theoretical advances in the computation of the phase diagram of colloid systems with Yukawa-like attractive potentials.²⁵ Though the protein solutions phase diagrams can be rationalized by this form of the potential energy, this model also does not provide a basis for a microscopic description of the interaction range for which it would be desirable to resort to a more detailed picture of the attractive interaction. More recently the correlation between the solubility and the second virial coefficient experimentally found for some protein systems has been interpreted by Haas et al.⁵ in terms of anisotropy of the protein–protein interactions that leads to the crystal arrangement and greatly determines the solubility.

Any attempt to characterize the range and type of the attractive protein–protein effective interaction is therefore a valuable improvement in the understanding of the protein–protein interactions, and this is the main aim of the paper. Our purpose is here to single out the most important features of the protein–protein specific interactions through the use of a simple van der Waals–electrostatic model that takes into account the nonspecific interactions with a mean field treatment. In doing so, we follow a usual description of the protein–protein interactions effects on light scattering^{21,26} just to make a zero-order approximation on which to build a more detailed picture. At this level, one imagines the protein as a hard dielectric sphere with uniform charge distribution and its most common analytical formulation is the so-called DLVO potential:³ a composition, $U_{\text{HA}}(r) + U_{\text{DH}}(r)$, of a short-range attractive interaction and a screened Coulomb repulsion. The short-range interaction is assumed to be described by the nonretarded form of the van der Waals dipolar interaction, known as the Hamaker potential^{3,6,27} given by

$$U_{\text{HA}}(r) = -\frac{H_A}{12} \left\{ \frac{4R^2}{r^2} + \frac{4R^2}{(r^2 - 4R^2)} + 2 \ln \left[\frac{r^2 - 4R^2}{r^2} \right] \right\} \quad (1)$$

where H_A is the Hamaker constant and R is the protein radius, $\sigma = 2R$. The calculated²⁸ protein–vacuum–protein interaction Hamaker constant is $H_A = 23.4 k_B T$ ($k_B = 1.38 \times 10^{-16}$ erg is the Boltzmann constant, and T is the absolute temperature) and the protein–water–protein $H_A = 3.1 k_B T$. It must be noted that other important short-range interactions, such as hydration forces^{12,17,29} or specific interactions, are not taken into account in the DLVO model and may enter in some effective way into the value of the Hamaker constant. The interaction described by eq 1 is singular at $r = 2R$ and its application needs the use^{6,15} of a cutoff, $r \geq \delta$. The choice of δ is not critical at low ionic strength where the Coulomb interactions dominate, however, already for moderate ionic strengths (≥ 100 mM), δ strongly correlates with the value of the Hamaker constant that fits the interaction data.^{15,30} We suggest that, from the microscopic point of view, this cutoff may be related to an extremely short-range repulsive interaction which adds to the van der Waals attraction: the result could be approximated by an attractive rectangular well as in the AHS model. As an example, close range repulsions have been studied in surface science experiments for some time³¹ and correlated to the repulsion between the hydration/counterions layer on approaching surfaces. Also in this case a mean-field approximation of the interaction between the protein surface atoms and the solvent molecules is assumed for simplicity.

Beside this hydration effect, at distances shorter than a nanometer (≈ 0.4 – 0.6 nm) the repulsion between the individual atoms of the two approaching proteins must come into play. A recent work on the interpretation of crystallographic data⁴ has estimated the contribution of these interactions by modeling them with a Lennard–Jones potential. The computation of the interaction energy over several protein crystals leads to the estimate of the short-range repulsive core as ≈ 0.1 – 0.15 nm (see Figures 5–8 of ref 4). This approach, valid at very short distances, puts into evidence the roughness and the details of the protein surfaces. Charged moieties may protrude from the average van der Waals protein

surface, and this picture is consistent with the possibility that a reduction of the attractive van der Waals attraction at very short distances arises actually from a displacement of the van der Waals surface from the charged protein surface.¹⁷

The electrostatic interaction $U_{DH}(r)$ is described by a Debye–Hückel screened Coulomb potential³

$$U_{DH}(r) = \frac{e_0^2 Q^2}{\epsilon(1 + \kappa_{DH}R)^2} \frac{\exp[-\kappa_{DH}(r - 2R)]}{r} \quad (2)$$

where ϵ is the solvent dielectric constant ($\epsilon = 78.5$ in water solutions³⁶ at 20 °C), Q is the number of net charges on the protein, e_0 is the proton charge ($e_0 = 4.8 \times 10^{-10}$ eu). The Debye screening κ_{DH} is computed according to the solution ionic strength, I_s , as $\kappa_{DH}^2 = 4\pi L_b I_s (1000 N_{av})$, where $L_b = 0.71$ nm (in water at 20 °C) is the Bjerrum length.³ To give a numerical example, at $I_s = 0.5$ M, the Debye screening is $\kappa_{DH} \approx 2.4 \times 10^7$ cm⁻¹. If a protein of the size of the lysozyme ($R \approx 1.8$ nm) brings a net charge $Q \approx 12$, the preexponential factor in eq 2 is $\approx 1.5 \times 10^{-20}$ erg cm. At the minimum approaching distance, $r = 2R$, we obtain then $U_{DH}(2R) \approx 4 \times 10^{-14}$ erg = $1 k_B T$. For comparison, at $I_s = 5$ M, we obtain $\kappa_{DH} \approx 7.5 \times 10^7$ cm⁻¹ and $U_{DH}(2R) \approx 5.6 \times 10^{-15}$ erg = $0.14 k_B T$.

III. Experiment

A. Proteins. Hen egg white lysozyme (MW 14300 Da) was purchased from Sigma (L6876, lot 57H7045) and used without further purification. The lyophilized compound was dissolved in sodium-acetate buffer (pH ≈ 4.2 , $I_s = 100$ mM) at concentration ≈ 30 g/L. Bovine betalactoglobulin B (MW 18400 Da) was purchased from Sigma (L8005, lot 13H7150) and dissolved in phosphate buffer (pH ≈ 7.8 , $I_s = 100$ mM) at concentration ≈ 30 g/L. All reagents were chemical grade.

We prepared the mother protein solutions at high protein concentration (≈ 30 g/L) and at the desired ionic strength of ammonium sulfate $(NH_4)_2SO_4$ just before light scattering measurements and diluted them by adding the appropriate amount of a stock of ammonium sulfate dissolved in the desired buffer (phosphate for BLG or acetate for lysozyme). The lysozyme mother solutions were prepared by adding small amounts of 3.5 M $(NH_4)_2SO_4$ while gently mixing the lysozyme solution with a magnetic stirrer, and keeping the solutions at ≈ 37 °C, to minimize ionic-shock induced large aggregates. Betalactoglobulin mother solutions were instead prepared by exhaustive dialysis against ammonium sulfate solution at concentrations gradually approaching the desired ionic strength. This was necessary in order to avoid massive aggregation and denaturation of this delicate protein. The ionic strength of the lysozyme solutions may be affected by the salt carried by the lyophilized protein. This contribution would increase I_s at most of ≈ 30 mM since the maximum concentration used for the experiments in the case of lysozyme is ≈ 16 g/L and the protein carries 28 charged residues. This implies at most a 15% error in the evaluation of the Debye length for the case when no ammonium sulfate is added to the solutions (buffer $I_s \approx 100$ mM). However this uncertainty is not relevant for the larger ionic strengths ($I_s \geq 600$ mM) on which we focus here.

The protein solutions and buffers were always filtered through a 0.2 μ m Millipore filter. The protein concentrations were determined after the scattering measurements by absorbance measurements at the excitation wavelength of 280 nm using extinction coefficients $\epsilon = 2.64$ L/(g cm) for lysozyme³² and $\epsilon = 0.96$ L/(g cm) for betalactoglobulin.³³ The solutions pH was always verified with a pHmeter to be pH ≈ 4.2 and pH ≈ 7.8 for lysozyme and betalactoglobulin, respectively.

For the protein partial molecular volumes we have used the values $v = 0.703$ mL/g for lysozyme^{7,30} and $v = 0.75$ mL/g for betalactoglobulin.³⁴

The protein volume can be obtained from the molecular weight and the partial molecular volumes. For lysozyme in monomeric forms, the volume $V = 16.8$ nm³ corresponds to a radius of the equivalent sphere, $R_M = 1.59$ nm. For the betalactoglobulin, the volume of the dimeric form that is found in solution at high salt content, is $V = 46$ nm³, which corresponds to an equivalent sphere of radius $R_M = 2.22$ nm.

B. Optical System. The laser source at 532 nm of the dynamic light scattering apparatus is a frequency doubled Nd:YVO₄ (1064 nm) diode-pumped laser (MillenniaII, Spectra Physics) in TEM₀₀ mode and has been kept at 1 W for the experiments reported here. The laser beam is spatially filtered and focused at the center of a quartz square cell having an optical path of 10 mm and a minimum working sample of 500 μ L. The scattered light can be collected at various angles by a lens and a multimode optical fiber mounted on a rotating arm. The output of the fiber is coupled to two distinct photomultipliers (H5873P-01, Hamamatsu) through a 50% beam splitter. The discriminated signals are sent to the two inputs of an ALV5000E/fast digital correlator (ALV, Langen, Germany) for the computation of the crosscorrelation functions. This setup allows the measurement of the autocorrelation function of the scattered light for lag times as short as 12.5 ns and has been described in detail elsewhere.³⁵

The experiments were performed at a temperature of 19.6 ± 0.1 °C. The sample temperature was measured by a thermocouple in close thermal contact with the bottom of the sample cell. The viscosity of the solutions are assumed to be equal to those of the solvent, η , obtained from the literature,³⁶ and the refractive index of the solutions have been measured by an Abbe refractometer with three significant digits and compared to the values obtained from the literature³⁶ in order to check for the salt concentration. The scattering angle θ is computed from the Snell law by employing the solution refraction index.³⁷

C. Photon Correlation Spectroscopy Data. The effect of the finite polymer volume fraction on the fluctuations of the scattered light intensity has been investigated theoretically and applied experimentally to several colloid systems and to protein solutions.^{3,6,38} These applications have been based on the analysis of the decay of the autocorrelation function of the scattered light. The normalized autocorrelation function of the light, $I(q, t)$, scattered from a monodisperse solution, is related to the mutual diffusion coefficient D by³⁹

$$g(\tau) = \frac{\langle I(q, t + \tau) I(q, t) \rangle_t}{\langle I(q, t) \rangle_t^2} = 1 + f_{coh} \exp[-\tau q^2 D] \quad (3)$$

where τ is the time difference and q the scattering vector equal to $(4\pi n/\lambda) \sin(\theta/2)$, n being the refracting index, λ the light wavelength, and θ the scattering angle. The coherence factor, $f_{coh} < 1$, is an instrumental constant determined by the collection optics,³⁷ and in the present measurements, $f_{coh} \approx 0.25$.

The translational diffusion coefficient D reflects the interactions between molecules at the first order in the protein mass concentration C (g/mL) as

$$D = D_0(1 + v k_D C) \quad (4)$$

where D_0 is the translational diffusion coefficient for vanishing protein–protein interactions, and it is related to the protein hydrodynamic radius R_h^0 via $D_0 = k_B T / (6\pi\eta R_h^0)$, where η is the solvent viscosity. The protein partial molecular volume is v . The protein mass concentration C is related to the volume fraction Φ as $\Phi = Cv$. The interaction constant k_D has no units since it multiplies the product of the concentration times the partial molecular volume. It is the result of an average over the protein–protein radial distribution function $g(r)$ of the hydrodynamic interactions according to

$$k_D = [k_D^{HS} + \int_{2R+\delta}^{\infty} (1 - g(r)) F(r) dr] \quad (5)$$

where R is the protein radius and δ is the integration cutoff needed to avoid the singularity of the Hamaker interactions. The hard core contribution to the interaction constant is given by k_D^{HS} whose value depends slightly on the particular treatment of the hydrodynamic interactions^{6,9} ranging between +1.56 and -0.9. The protein-protein radial distribution function is, to the first-order approximation in the protein concentration, $g(r) = \exp(-U_{\text{DLVO}}(r)/k_B T)$ and we have employed the distance dependence $F(r)$ of the hydrodynamic interaction given by Batchelor:⁴⁰

$$F(r) = -0.706 - 11.89\left(\frac{r}{2R}\right) + 1.69\left(\frac{r}{2R}\right)^{-1} + 24\left(\frac{r}{2R}\right)^2 \quad (6)$$

Alternative analytical forms of the hydrodynamic interactions⁶ have been given, though all of them give nearly the same numerical description.⁹ The interaction constant k_D is positive for repulsive interactions and assumes negative values when relevant attractive interactions occur.

D. Data Analysis. For all the measurements the baseline corresponds to $\approx 10^8$ photon counts. The autocorrelation functions of the scattered light are successfully fit to a single-exponential decay (eq 3) by means of the nonlinear least-squares fitting Levenberg-Marquardt algorithm.⁴¹ The second-order cumulant analysis⁴² gives an average polydispersity $\approx 0.06 \pm 0.012$ for the betalactoglobulin solutions over all the protein and ammonium sulfate concentrations. Analogously, we find for the lysozyme solutions an average polydispersity $\approx 0.055 \pm 0.015$. These values of the polydispersity do not correspond to essentially monodisperse solutions, and the presence of small aggregates cannot be ruled out. However the amount of aggregates should be low since the autocorrelation functions for betalactoglobulin and lysozyme solutions have been satisfactorily analyzed as a single-exponential decay showing no systematic oscillation in the residuals.

The evaluation of the interaction constant, k_D , has been performed by numerically integrating eq 5 by means of a refinement of the routines QTRAP and TRAPZD from Numerical Recipes.⁴³

IV. Results

The autocorrelation functions of the scattered light from lysozyme and betalactoglobulin solutions have been measured at several protein concentrations C in the range 1–30 g/L and for ammonium sulfate ionic strengths I_s in the range 600 mM to 6 M. The results obtained on the lysozyme solutions are taken as a reference for the experiments on the solutions of betalactoglobulin whose crystallization conditions are less studied.

Preliminary measurements of the diffusion coefficient D have been performed at few (usually 3 or 4) concentrations for several scattering vectors in the range $2.8 \times 10^{10} \text{ cm}^2/\text{s} \leq q^2 \leq 7 \times 10^{10} \text{ cm}^2/\text{s}$ in order to check for the angular dependence of the diffusion coefficient. Figure 1 shows for example a typical dynamic Zimm plot³⁰ obtained for lysozyme at $I_s = 2.4 \text{ M}$. In this graph the diffusion coefficient D is plotted vs the parameter $q^2 + \alpha C$, which depends on both scattering vector q and protein concentration. The extrapolated value of D at $C \approx 0$ and $q^2 \approx 0$ is the infinite dilution translational diffusion coefficient D_0 given in eq 4. The measured values of D show little (or no) dependence on the magnitude of the scattering vector q as expected for particles whose size is much smaller than the wavelength of the light, such as lysozyme and betalactoglobulin, confirming that samples in these experiments do not contain large aggregates. Therefore, all the other measurements of the diffusion coefficient D have been performed at a fixed angle $\theta = 90^\circ$ and for several (10 or more) protein concentrations.

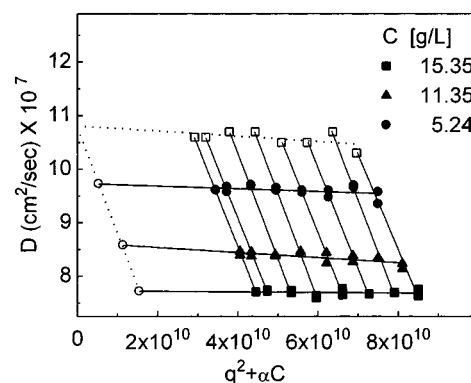


Figure 1. Dynamic Zimm plot for lysozyme in ammonium sulfate: ionic strength = 2.4 M, pH = 4.2 (0.1 M acetate buffer). Filled symbols correspond to the protein concentrations $C = 5.2$ (circles), 11.3 (triangles), and 15.3 g/L (squares). The open squares and circles refer to the extrapolation of D to $C \approx 0$ and to $q^2 \approx 0$. D_0 is given by the intersection of the linear fits (dotted lines) through the extrapolated D values. The plotting constant is $\alpha = 10^9$.

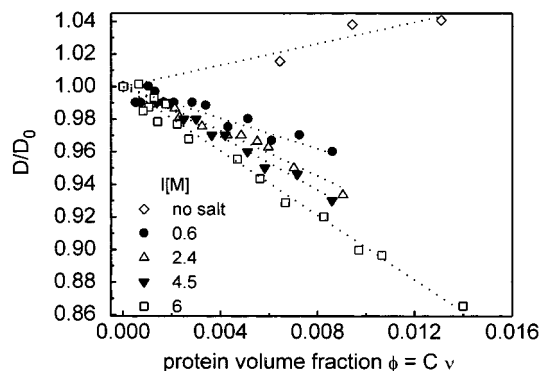


Figure 2. Normalized mutual diffusion coefficient D/D_0 of betalactoglobulin in ammonium sulfate solutions vs the protein volume fraction at pH = 7.8, 0.05 M phosphate buffer. The different symbols refer to ionic strengths in the range 0.6–6 M as indicated in the plot.

The diffusion coefficient D measured vs the protein concentration C at all the investigated ionic strengths is very well described by a linear relation for both proteins. Figure 2 shows, as an example, the normalized diffusion coefficient D/D_0 for betalactoglobulin solutions at various values of the ionic strength I_s together with a linear fit to the data. Moreover, the dependence of the infinite dilution diffusion coefficient, D_0 , on the ionic strength (see Table 1) is mainly due, for both proteins, to the increase of the solvent viscosity η . In fact (Table 1) the hydrodynamic radii obtained via the Stokes-Einstein relation $D_0 = k_B T / (6\pi\eta R_h)$, are fairly constant. The average value of the hydrodynamic radius is $R_h = 1.80 \pm 0.1 \text{ nm}$ for lysozyme and $R_h = 2.75 \pm 0.2 \text{ nm}$ for betalactoglobulin, in agreement with those reported previously.^{30,44,45} The translational diffusion coefficient D_0 has been computed by de la Torre et al.⁴⁶ for lysozyme (entry:6lyz; www.rcsb.org/pdb/, type EC 0.3.2.1.17) and for betalactoglobulin (entry:1beb; www.rcsb.org/pdb/) with a method that describes in detail the exact shape of the protein and takes into account also for the hydration of the surface amino acids. Similar approaches have been previously presented in the literature⁴⁷ and applied to lysozyme, finding results very similar to those reported by de la Torre et al.⁴⁶ The outcome of this computation shows a very good agreement with our experimental results in the absence of

Table 1. Infinite Dilution Diffusion Coefficient and Hydrodynamic Radii for the Lysozyme and the Betalactoglobulin Solutions^a

I_s (M)	η/η_0	$D_0 \times 10^7$ (cm ² /s)	R_h (nm)
Betalactoglobulin			
0	1.010	8.1	2.59
0.6	1.042	7.89	2.58
2.4	1.151	6.15	2.99
4.5	1.351	5.48	2.86
6	1.543	4.99	2.75
Lysozyme			
0	1.010	11.3	1.86
1.2	1.072	10.3	1.92
2.4	1.151	10.5	1.74
4.8	1.386	8.8	1.74

^a I_s is the ammonium sulfate ionic strength. The values for the viscosity of the solutions η relative to the water viscosity η_0 at $T = 19.6^\circ\text{C}$ as a function of ammonium sulfate ionic strength were taken from the literature.³⁶

ammonium sulfate. For lysozyme we find $D_0 = 11.9 (\pm 2) \times 10^{-7}$ cm²/s, to be compared to the predicted value $D_0 = 11.2 \times 10^{-7}$ cm²/s (for 6lyz)⁴⁶ and for betalactoglobulin we measure $D_0 = 7.8 (\pm 0.6) \times 10^{-7}$ cm²/s, to be compared to the predicted value $D_0 = 7.81 \times 10^{-7}$ cm²/s (1beb).⁴⁶

The isotropic picture of the protein shape is certainly inadequate though the values of R_h do roughly correspond to the radius R_M (see Proteins section) plus some hydration layer. However, for lysozyme solutions the difference between R_h and R_M corresponds to a hydration layer¹⁵ $\approx 0.2 \pm 0.1$ nm while for the dimeric form of betalactoglobulin $R_h - R_M \approx 0.5 \pm 0.2$ nm. This difference cannot be regarded as a real change in the hydration of the two proteins, but it arises from the shape anisotropy and is fully taken into account by computations based on the protein crystal structure.^{46,47}

It is important to notice that, although very well described by a linear relation, the data in Figure 2 might also be compatible with a smooth aggregation at increasing protein concentration, since both attractive interactions between the proteins and aggregations lead to a decrease of the apparent diffusion coefficient.^{9,38} However extensive aggregation does not seem to occur since no evident dependence of the diffusion coefficient on the scattering angle is found when studying the dynamic Zimm plot as shown for example in Figure 1. Moreover, the behavior of the apparent mutual diffusion coefficient vs the protein concentration for the case of a reversible dimerization of proteins is different from the observed linear decrease.^{9,38} The value ≈ 0.06 of the polydispersity indicates that small amounts of low molecular weight aggregates may occur. However no evident increase of the polydispersity with the protein and the ammonium sulfate concentration is found, indicating that any form of initial aggregation in the protein solution does not vary appreciably with the addition of the ammonium sulfate or the increase in the protein concentration. Typical values of the polydispersity obtained with a second-order cumulant analysis^{42,48} are reported in Figure 3 for lysozyme and betalactoglobulin. The uncertainty in the polydispersity does not allow to find a clear trend of this parameter with the protein concentration.

We have determined the interaction constants k_D (eqs 4 and 5) from the slope of the linear fit of the mutual diffusion D vs protein concentration C at each ionic strength. As summarized in Figure 4 the interaction coefficients k_D decrease with I_s , indicating an increase

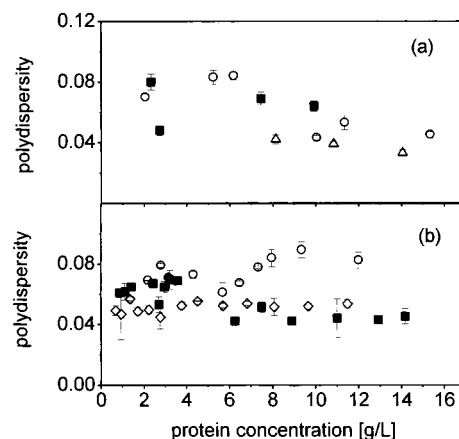


Figure 3. Polydispersity obtained from a second-order cumulant analysis of the autocorrelation functions of the scattered light reported vs the protein concentration. Panel a: lysozyme solutions at ammonium sulfate concentration $[(\text{NH}_4)_2\text{SO}_4] = 0.8$ M (open triangles), $[(\text{NH}_4)_2\text{SO}_4] = 0.8$ M (open circles), and $[(\text{NH}_4)_2\text{SO}_4] = 1.6$ M (filled squares). Panel b: betalactoglobulin solutions at ammonium sulfate concentration $[(\text{NH}_4)_2\text{SO}_4] = 0.2$ M (open diamonds), $[(\text{NH}_4)_2\text{SO}_4] = 0.8$ M (open circles), and $[(\text{NH}_4)_2\text{SO}_4] = 2.0$ M (filled squares).

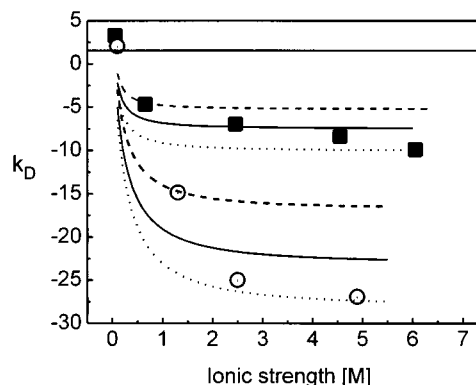


Figure 4. Experimental interaction constants k_D (dimensional, see text) vs ammonium sulfate ionic strength for betalactoglobulin (filled squares) and lysozyme (open circles). Curves are predictions made with the DLVO model with the minimum (dotted), average (solid) and maximum (dashed) values obtained for δ from Figure 5. For betalactoglobulin, $Q = 12$, $H_A = 4kT$, and $\delta = 0.147, 0.162$, and 0.185 respectively, while for lysozyme $Q = 10$, $H_A = 8kT$, and $\delta = 0.144, 0.150$, and 0.164 . The horizontal line indicates the hard core contribution k_D^{HS} value.

in the attractive interactions, for both proteins. It is worth noting that the initial dependence of k_D vs I_s is steeper for lysozyme than for betalactoglobulin and at high I_s the lysozyme–lysozyme interactions are approximately twice as large as those of the betalactoglobulin.

V. Discussion

The experimental data can be directly compared to the predictions made according to the interaction model by numerically computing eq 5. In the following, we are employing the DLVO model that in our opinion can describe the behavior of the interaction constant and may help in shedding some light on the balance between attractive and repulsive interactions at very short range. However this model is not meant to fully take into account all the complex protein–protein interactions that eventually may lead to aggregation or crystallization.

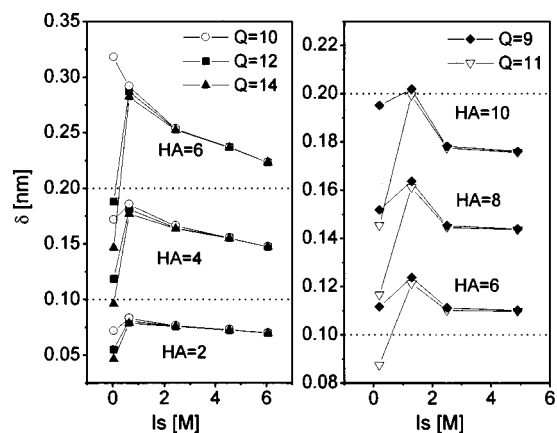


Figure 5. Values of the best fit cutoff, δ , vs the ionic strengths for betalactoglobulin (left panel) and lysozyme (right panel) obtained by fitting the interaction constant plotted in Figure 4. The values of the Hamaker constant and of the protein charge are indicated in the plot.

The model parameters are the protein radius, R , its charge Q , the Hamaker constant, and cutoff distance δ whose role, within the DLVO model, is simply that of avoiding the singularity of the Hamaker interaction energy. Beside the protein physical parameters, the computation of the interaction constant must also take into account the hard sphere contribution,^{6,9} which is assumed here to be $k_D^{\text{HS}} = 1.56$. A slightly altered value might affect the analysis of the data at most at the lower ionic strengths. Regarding the choice of the parameters, the protein radii are assumed $R_{\text{Lys}} = 1.8$ nm for lysozyme and $R_{\text{BLG}} = 2.75$ nm for the betalactoglobulin dimer as computed from the extrapolation of the diffusion coefficient at vanishing protein concentration in the Results section. Tentative values of the protein charge Q and the Hamaker constant can be argued from previous works. In particular, the protein charge depends on the solution pH and has been directly measured by titration methods from which we assume $Q \approx +12$ for lysozyme⁴⁹ at $\text{pH} \approx 4$ and $Q = -12$ for the dimer of betalactoglobulin⁵⁰ $\text{pH} \approx 8$. The choice of the Hamaker constant is less definite. Direct measurements⁵¹ of H_A in protein systems give values close to $k_B T$, and theoretical estimates indicate values close to $3 k_B T$ for globular proteins.⁵² However when using the DLVO interaction model to fit the results of either static light scattering (second virial coefficient) or photon correlation spectroscopy measurements, one finds larger values of H_A , usually in the range $1\text{--}10 k_B T$. For lysozyme, as an example, values from 4 to $11 k_B T$ are reported,^{15,21,26} while for betalactoglobulin we have previously found³⁸ values $H_A \approx 5 k_B T$. This range of experimental values for H_A can be ascribed to the approximations embedded in the DLVO treatment of short range interactions that are modeled only as van der Waals attractions. In fact, most of the short range interactions are simply described by the Hamaker potential and by the cutoff at $r \geq \delta$. The fitting parameter H_A plays therefore a role different from the original one related only to the dipolar attraction.

At first we have fit the experimental behavior of k_D vs I_s , by fixing R and Q as discussed above, by assuming different values of H_A in the range $2 k_B T \leq H_A \leq 10 k_B T$ and by leaving as a free parameter the cutoff δ reported in Figure 5. As can be seen from this figure, the computation of k_D is affected by the choice of the protein charge only at the lower values of the ionic strength

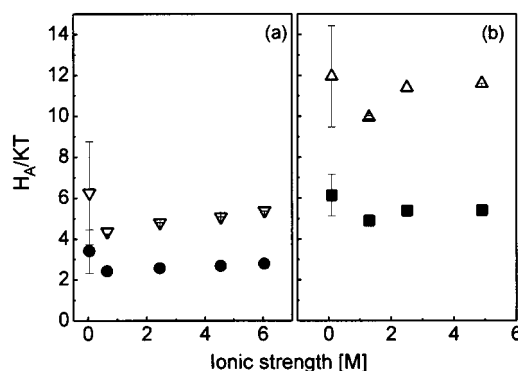


Figure 6. Values of the best fit H_A obtained from the fit of k_D vs the ionic strength with a DLVO model of the interactions, for betalactoglobulin (left panel) and lysozyme (right panel). The protein charges and radii are $Q = 12$, $R_h = 2.75$ nm and $Q = 10$, $R_h = 1.8$ nm for betalactoglobulin and lysozyme, respectively. Two values of the cutoff shell δ are assumed: $\delta = 0.1$ nm (filled squares), and $\delta = 0.2$ nm (open circles).

where the counterions screening length is larger and our choice for the protein charges does not seem to affect the overall trend of δ with the ionic strength. The best fit δ shows a slight decrease with I_s whose effect is evident also in Figure 4 where the simulations obtained for the minimum, the average, and the maximum value of δ observed in Figure 5 are shown as lines. While the experimental data show a slow descent, the best fitting curves are approaching a definite plateau value. Sources for the apparent change of the cutoff δ observed in Figure 5 may be found, for example, in the salt-induced dehydration of the protein surface or some other desorbing process. In any case, the present values of the cutoff δ for lysozyme and betalactoglobulin are well within the range reported by other groups: Farnum et al.¹⁵ use 0.1 nm for lysozyme in glycerol–NaCl solutions, Baldini et al.³⁸ assume $\delta \approx 0.2$ nm for betalactoglobulin in NaCl solutions, and Kuehner et al.³⁰ investigate the correlation between H_A and δ and assume $\delta = 0.08$ nm for the data analysis of lysozyme in either NaCl or $(\text{NH}_4)_2\text{SO}_4$ solutions.

Therefore, the trend of k_D vs I_s can be accounted for by a 20–30% decrease in the cutoff shell, δ . However, since we are investigating two different proteins in solutions of the same salt, ammonium sulfate, a common value for the average minimum approaching distance for the two proteins could be reasonably expected in the range $0.1 \text{ nm} \leq \delta \leq 0.2 \text{ nm}$. In Figure 6 we report the H_A values obtained from the analysis of k_D vs the ionic strength with a single value of δ . In this case, we have assumed either $\delta = 0.1$ nm or $\delta = 0.2$ nm, finding that the Hamaker constant is nearly twice higher for lysozyme than for betalactoglobulin. The variation of the fitting parameter, H_A , with the ionic strength observed in Figure 6 is smaller than the systematic 20–30% decrease of δ with I_s reported in Figure 5, indicating that the interaction constant is more sensitive to changes in H_A than in δ .

Apart from these minor solvent-induced changes in the dipolar interactions for both proteins, the larger value of the Hamaker constant observed for lysozyme in Figure 6 is a further indication of a larger effective attractive short-range interaction for this protein than for betalactoglobulin. Additional specific or unspecific short-range interactions that go beyond the DLVO description and need a microscopic picture of the proteins are the origin for the difference between

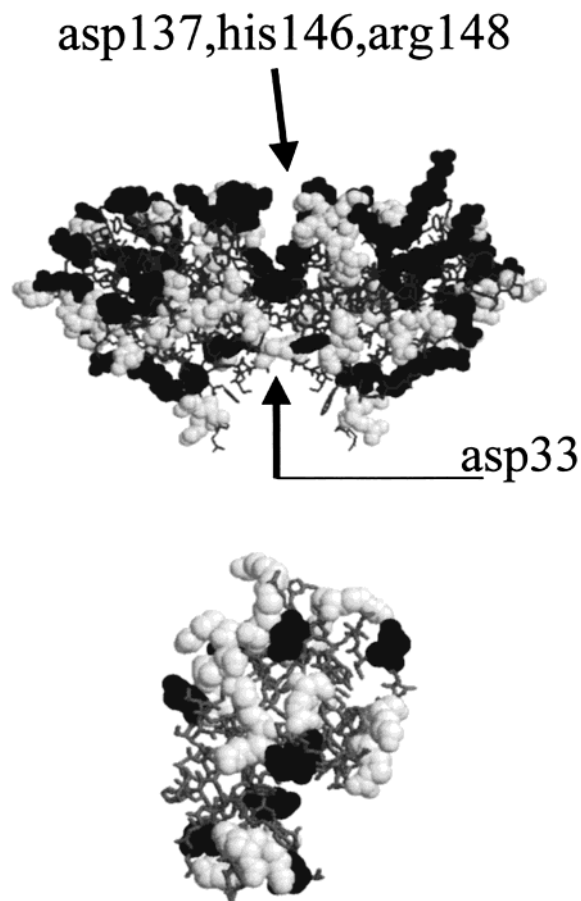


Figure 7. Betalactoglobulin dimer (top) and lysozyme (bottom) molecules, as obtained from PDB files: 1beb and 6lyz, respectively (Protein Data Bank, www.rcsb.org/pdb/) Basic and acidic amino acid residues are shown in a space-filling presentation in light and dark gray respectively, the remainder of the molecule is shown as sticks. For betalactoglobulin protein, charged residues buried at the monomer–monomer interface are indicated in the plot.

lysozyme and betalactoglobulin interactions. As a matter of fact, we could not in any case account for the ratio ≈ 2 between the average H_A values for lysozyme and for betalactoglobulin just by considering the dependence⁵³ of $H_A \div v^{-2}$ on the partial molecular volume v predicted by the classical DLVO model. The slight change in the partial molecular volume of the two proteins, from 0.70 mL/g for lysozyme to 0.75 mL/g for betalactoglobulin, would give only a factor of ≈ 1.15 in the ratio of the Hamaker constants.

Indeed, the two proteins have different charges at the pH values used for the present experiments. Lysozyme has a net positive charge, $Q \approx +12$ with a surface density $\approx 0.47 \text{ nm}^{-2}$, while the betalactoglobulin dimer has a net negative charge, $Q \approx -12$, with a surface density $\approx 0.23 \text{ nm}^{-2}$. On the other hand, regarding the total number of charges, lysozyme has ≈ 28 charged residues at pH ≈ 4 , while betalactoglobulin at pH ≈ 8 shows ≈ 44 charges per monomer. Again the number of charges per unit surface of the two proteins is not very large: $\approx 0.9 \text{ nm}^{-2}$ for lysozyme and $\approx 1.3 \text{ nm}^{-2}$ for betalactoglobulin when also taking into account the charged residues buried in the monomer–monomer interface (Figure 7). Therefore, the two proteins do not show large differences in terms of net charge and in the number of charged residues per surface unit. Similar results are found when analyzing the number of resi-

dues capable of performing hydrogen bonding on the two proteins.

However, proteins are zwitterions, and the net charge is always due to the balance between different numbers of positively and negatively charged residues. As a matter of fact, the net positive charge of lysozyme at pH ≈ 4 is mostly due to the charged basic residues (≈ 18 out of 28), while the betalactoglobulin dimer has, at pH ≈ 8 , very similar numbers of charged basic (≈ 17) and acidic residues (≈ 24). This can be seen from Figure 7 where the basic and acidic amino acid residues are shown as light and dark gray space-filled atoms, respectively. This charge imbalance means that a larger number of positive hydrated counterions, ammonium ions, are condensed around betalactoglobulin than around lysozyme. We expect, therefore, that the disruption of the hydration layer around betalactoglobulin needed to bring proteins to a very short distance is more difficult for betalactoglobulin than for the lysozyme. This would lead to larger repulsive hydration forces for betalactoglobulin than for lysozyme or, from another point of view, to a weaker attractive interaction as shown from the values of the Hamaker constant in Figure 6. Even in a mean-field approximation the exact dependence of the hydration energy on the ionic strength does not seem to be available. The following empirical and approximated relation has been proposed and widely applied:^{12,53}

$$U_{\text{hyd}}(r) = \pi f_0 R L \exp[-(r - 2R)/L] \quad (7)$$

We are not aware of simpler relations for the hydration interaction energy. The application of eq 7 to such complex and anisotropic systems as proteins has however intrinsic profound limitations. Surface force measurements give $f_0 \approx 0.75 - 7.5 k_B T/\text{nm}^2$ and $L \approx 0.6 - 1.1 \text{ nm}$. Apart from the protein radius in the preexponential factor, the dependence on the protein properties, such as the extent of its hydration, is embedded in the term f_0 . A rough estimate of the effect of the hydration term in the present case can be obtained by assuming that the observed difference ΔU_δ in the interaction energy at the minimum approaching distance for lysozyme and betalactoglobulin is entirely due to the hydration forces, while the van der Waals interactions are described by a common value of H_A for both proteins. As an example we find from the fitting of k_D a value of $\Delta U_\delta \approx 1.4 k_B T$ by assuming $\delta = 0.1 \text{ nm}$. This difference can be accounted for by the smaller hydration repulsion on lysozyme, $f_0 \approx 0.7 k_B T/\text{nm}^2$, than on betalactoglobulin, $f_0 \approx 5.7 k_B T/\text{nm}^2$, when assuming, e.g., $L = 0.6 \text{ nm}$ and $H_A = 6 k_B T$. These values of f_0 are in good agreement with those previously reported in the literature¹² and suggest that the observed difference in the effective attractive interactions of these two proteins might be interpreted in a mean-field picture as being due to a weaker hydration repulsion in lysozyme than in betalactoglobulin. According to the simple eq 7, this should be determined by the smaller radius of lysozyme and by the smaller amount of condensed positively charged hydrated ions on lysozyme than on betalactoglobulin.

VI. Conclusions

We have characterized the strength of the protein–protein interactions for lysozyme and betalactoglobulin in ammonium sulfate solutions by measuring the steepness of the dependence of the mutual diffusion coef-

ficient on the ionic strength. Though similar in shape and size, the two proteins show distinct interaction properties, and lysozyme interacts more strongly than betalactoglobulin. We have assumed the DLVO potential with a common value of the minimum approaching distance, δ , only to have a zero-order level of description on which a more detailed picture could be drawn. We find that the Hamaker constant is nearly twice as large in lysozyme than in betalactoglobulin at the same ammonium sulfate concentration. This finding does not seem to be directly related to the presence of dramatically larger number of residues on the protein surface. On the other hand, the larger condensation of positively hydrated counterions on betalactoglobulin, and the larger size of the betalactoglobulin dimer, may be the origin of larger repulsive hydration forces for betalactoglobulin that show up as a smaller effective van der Waals attractive interaction.

Acknowledgment. This research was supported by the Advanced Research Project "PROCRY" grant of the Istituto Nazionale per la Fisica della Materia (INFM). Thanks are due to Giovanna Fedele for help with the measurements.

References and Notes

- (1) Denton, A. R.; Lowen, H. *Phys. Rev. Lett.* **1998**, *81*, 469–472.
- (2) Kierzek, A. M.; Wolf, W. M.; Zielenkiewicz, P. *Biophys. J.* **1997**, *73*, 571–580.
- (3) Nägele, G. *Phys. Rep.* **1996**, *272*, 215–372.
- (4) Asthagiri, D.; Neal, B. L.; Lenhoff, A. M. *Biophys. Chem.* **1999**, *78*, 219–231.
- (5) Haas, C.; Drenth, J.; Wilson, W. W. *J. Phys. Chem. B* **1999**, *103*, 2808–2811.
- (6) Corti, M.; Degiorgio, V. *J. Phys. Chem.* **1981**, *85*, 711–717.
- (7) Piazza, R.; Peyre, V.; Degiorgio, V. *Phys. Rev. E* **1998**, *58*, R2733–R2736.
- (8) Dhont, J. K. G. *An Introduction to Dynamics of Colloids*; Elsevier: Amsterdam, 1996.
- (9) Beretta, S.; Chirico, G.; Arosio, D.; Baldini, G. *J. Chem. Phys.* **1997**, *106*, 8427–8435.
- (10) Sear, R. P. *J. Chem. Phys.* **1999**, *111*, 4800–4806.
- (11) Neal, B. L.; Asthagiri, D.; Velev, O. D.; Lenhoff, A. M.; Kaler, E. W. *J. Cryst. Growth* **1999**, *196*, 377–387.
- (12) Petsev, D. N.; Vekilov, P. G. *Phys. Rev. Lett.* **2000**, *84*, 1339–1342.
- (13) McPherson, A. *Preparation and Analysis of Protein Crystals*; Wiley: New York, 1992.
- (14) Mahadevan, H.; Hall, C. K. *Am. Inst. Chem. Eng. J.* **1990**, *36*, 1517–1528.
- (15) Farnum, M.; Zukoski, C. F. *Biophys. J.* **1999**, *76*, 2716–2726.
- (16) Muschol, M.; Rosenberg, F. *J. Chem. Phys.* **1997**, *107*, 1953–1962.
- (17) Israelachvili, J. N.; Wennerstrom, H. *Nature* **1996**, *379*, 219–225.
- (18) George, A.; Wilson, W. W. *Acta Crystallogr. D* **1994**, *50*, 361–365.
- (19) Poon, W. C. K. *Phys. Rev. E* **1997**, *55*, 3762–3764.
- (20) Rosenbaum, D. F.; Zamora, P. C.; Zukoski, C. F. *Phys. Rev. Lett.* **1996**, *76*, 150–153.
- (21) Muschol, M.; Rosenberg, F. *J. Chem. Phys.* **1995**, *103*, 10424–10432.
- (22) Rosenbaum, D. F.; Kulkarni, A.; Ramakrishnan, S.; Zukoski, C. F. *J. Chem. Phys.* **1999**, *111*, 9882–9890.
- (23) Baxter, R. J. *J. Chem. Phys.* **1968**, *49*, 2770–2774.
- (24) Fine, B. M.; Lomakin, A.; Benedek, G. B. *J. Chem. Phys.* **1996**, *104*, 326–335.
- (25) Hagen, M. H. J.; Frenkel, D. *J. Chem. Phys.* **1994**, *101*, 4093–4097.
- (26) Eberstein, W. Y.; Georgalis, Y.; Saenger, W. *J. Cryst. Growth* **1994**, *143*, 71–78.
- (27) Hough, D. B.; White, L. R. *Adv. Colloid. Interface Sci.* **1980**, *14*, 3–41.
- (28) Roth, C. M.; Neal, B. L.; Lenhoff, A. M. *Biophys. J.* **1996**, *70*, 977–987.
- (29) Kornyshev, A. A.; Kossakowski, D. A.; Leikin, S. *J. Chem. Phys.* **1992**, *97*, 6809–6820.
- (30) Kuehner, D. E.; Heyer, C.; Rämisch, C.; Fornefeld, U. M.; Blanch, H. W.; Prausnitz, J. M. *Biophys. J.* **1997**, *73*, 3211–3224.
- (31) Kjellander, R.; Marcelja, S.; Pashley, R. M.; Quirk, J. P. *J. Chem. Phys.* **1990**, *92*, 4399–4407.
- (32) Sophianopoulos, A. J.; Rhodes, C. K.; Holcomb, D. N.; Van Holde, K. E. *J. Biol. Chem.* **1962**, *237*, 1107–1112.
- (33) Townend, R.; Winterbottom, R. J.; Timasheff, S. N. *J. Am. Chem. Soc.* **1960**, *82*, 3161–8.
- (34) Tanford, C. *Physical Chemistry of Macromolecules*; Wiley: New York, 1961.
- (35) Chirico, G.; Gardella, M. *Appl. Opt.* **1999**, *38*, 2059–2067.
- (36) Weast, R. C.; Astle, M. J. *CRC Handbook of Chemistry and Physics*, 63 ed.; CRC: Boca Raton, FL, 1982–1983.
- (37) Chu, B. *Laser Light Scattering: Basic Principles and Practice*, 2nd ed.; Academic Press: San Diego, CA, 1991.
- (38) Baldini, G.; Beretta, S.; Chirico, G.; Franz, H.; Maccioni, E.; Mariani, P.; Spinazzi, F. *Macromolecules* **1999**, *32*, 6128–6138.
- (39) Berne, B. J.; Pecora, R. In *Dynamic Light Scattering*; Wiley: New York, 1976.
- (40) Batchelor, J. K. *J. Fluid. Mech.* **1976**, *74*, 1–29.
- (41) Bevington, P. R. *Data Reduction and Error Analysis for the Physical Sciences*, 1st ed.; McGraw-Hill: New York, 1969.
- (42) Koppel, D. E. *J. Chem. Phys.* **1972**, *57*, 4814–4820.
- (43) Press, W. H.; Teukolsky, S. A.; Vetterling, W. T.; Flannery, B. P. *Numerical Recipes in C: The Art of Scientific Computing*, 2nd ed.; Cambridge University Press: New York, 1993.
- (44) Aymard, P.; Durand, D.; Nicolai, T. *Int. J. Biol. Macromol.* **1996**, *19*, 213–221.
- (45) Aymard, P.; Nicolai, T.; Durand, D.; Clark, A. *Macromolecules* **1999**, *32*, 2542.
- (46) De la Torre, J. G.; Huertas, M. L.; Carrasco, B. *Biophys. J.* **2000**, *78*, 719–730.
- (47) Brune, D.; Kim, S. *Proc. Natl. Acad. Sci. U.S.A.* **1990**, *90*, 3835–3839.
- (48) Beretta, S.; Chirico, G.; Lunelli, L.; Baldini, G. *Appl. Opt.* **1996**, *35*, 3763–3770.
- (49) Tanford, C.; Wagner, M. L. *J. Am. Chem. Soc.* **1954**, *76*, 3331.
- (50) Bash, J. J.; Timasheff, S. *Arch. Biochem. Biophys.* **1967**, *118*, 37–47.
- (51) Leckband, D. E.; Schmitt, F. J.; Israelachvili, J. N.; Knoll, W. *Biochemistry* **1994**, *33*, 4611–4624.
- (52) Nir, S. *Prog. Surf. Sci.* **1976**, *8*, 1–58.
- (53) Israelachvili, J. N. In *Intermolecular and Surface Forces*, 2nd ed.; Academic Press: London, 1992.

MA0006171